$$F_V \quad \frac{1}{2\sqrt{V}} \begin{pmatrix} 2V_x & V_y \\ V_y & V_x \\ -6W_{xy} & \end{pmatrix} \qquad (3)$$

Thus the eigenpairs influenced by the physical nonlinearity are calculated. The fifth eigenmode is shown in Fig.2. The statically distorted mesh is gray while the eigenmode is black.

Fig. 2. The fifth eigenmode (the statically distorted mesh is gray while the eigenmode is black)

The equivalent stress:

$$\sqrt{\frac{1}{3}(V_x \quad V_y)^2 \quad \frac{1}{3}V_x V_y \quad W_{xy}^2} \qquad (4)$$

represented by intensity mapping of the type proposed in [3] is shown in Fig. 3.

Better continuity is achieved by smoothing the stresses and calculating the equivalent stress on their basis. The equivalent stress represented by intensity mapping with the application of smoothing is shown in Fig. 4.

Fig. 3 and 4 serve as an approximate reference for judging about the possible shapes of the nonlinear plasticity region.

The stroboscopic moire fringes for the seventh eigenmode are represented in Fig.5. The problem of their interpretation is that the moire grating is regular in the status of equilibrium. When the control parameter is non-zero, the structure undertakes linear deformations what distorts the grating. Only after this, the image of deformed structure performing eigen vibrations is superimposed with the image of the statically loaded structure. It can be noted that such visualisation brings useful information about the shape of vibrations but is not applicable for detection of zones of plasticity in the analyzed structure.

The moire fringes obtained as a superposition of the linear system and system undertaking physical nonlinearity are shown in Fig.6. Such analysis does not bring into account the shape of the eigenvibrations, but instead provides an insight into the effect of nonlinearity.

Investigation of the plate bending problem

The rectangular plate of the thickness h is analyzed using the element of the type described in [2]. The components of the stresses W_{xz}, W_{yz} in the further analysis are assumed to be small and related with the corresponding components of the strains elastically. The lower and upper boundaries are fastened and the upper one is kinematically displaced in the direction of the z axis. The static problem is solved. The regions of the surface of the plate where the equivalent stress given by Eq.1 is greater or equal than a predefined value are assumed to be in a plastic state. The statically distorted mesh with the points of numerical integration in the plastic state at the surfaces of the plate is shown in Fig. 7. The mesh in the status of equilibrium is gray, while the statically distorted mesh in the cavalier projection [4, 5] with an angle $\alpha = 45°$ is black.

F

Fig. 3. The equivalent stress represented by intensity mapping

Fig.4. The equivalent stress represented by intensity mapping with smoothing

Fig. 5. The stroboscopic moire fringes for the seventh eigenmode

Fig. 6. The moire fringes obtained as a superposition of the linear system and the one taking the nonlinearity into account for the second eigenmode

Fig. 7. The mesh in the status of equilibrium (shown in gray) and the statically distorted mesh in the cavalier projection with the points of numerical integration in the plastic region

The stiffness and mass matrixes are calculated by taking the elastic-plastic matrix of elastic constants for those points of numerical integration that are in the plastic region at the surfaces of the plate into account. The thickness of the internal elastic layer he is determined. The following notation is introduced:

$$D_{ep} \quad D \quad D_T , \tag{5}$$

where:

$$D_T \quad \frac{DF_V (DF_V)^T}{\frac{EE_T}{E \quad E_T} \quad F_V^T DF_V} . \tag{6}$$

Then in the part of the stiffness matrix related with the components of the stresses V_x, V_y, V_{xy} the terms dependent on the z coordinate are D_{ep} multiplied by z squared. This results in:

$$\int_{-\frac{h}{2}}^{\frac{h}{2}} D_{ep} z^2 dz \quad D \frac{h^3}{12} \quad D_T \left(\frac{h^3}{12} \quad \frac{h_e^3}{12} \right). \tag{7}$$

Thus the eigenpairs influenced by the physical nonlinearity are calculated.

The equivalent stress given by Eq. 4 represented by intensity mapping with the application of smoothing is shown in Fig. 8. On the basis of this figure one can approximately judge about the possible shapes of the nonlinear region at the surfaces of the plate.

Fig.8. The equivalent stress represented by intensity mapping with smoothing

Control of eigenfrequencies

Finally, the relation between the scaled eigenfrequences and the control parameter (static shift of the upper boundary) is presented in Fig. 9. It can be clearly seen that though the eigenfrequencies start decreasing around the same value of the control parameter, the slope of different eigenfrequencies is quite distinct. It can be noted that the value of the first eigenfrequency is scaled to unity for better interpretability of results.

It can be noted that though the presented control methodology is well applicable for the first natural eigenfrequency, but in practice this technique can be used for higher modes in predefined ranges of frequencies thus enabling the solution of advanced multi-body interaction problems.

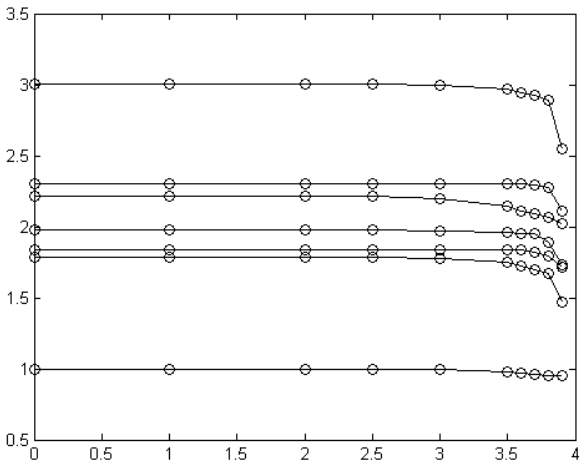

Fig.9. The relationship of the eigenfrequency divided by the first eigenfrequency with the displacement of the upper boundary for the first seven eigenfrequencies

Conclusions

Numerical procedure for analysis of eigenmodes and eigenfrequencies influenced by static physical nonlinearity is proposed.

This method of statical control of eigenfrequencies on the basis of physical nonlinearity is applicable in the design of vibrational mechanisms.

It is shown that double exposure geometric moire techniques are applicable for identification of zones of plasticity.

References

1. Barauskas R. Basis of the finite element method. Kaunas: Technologija. 1999. P. 376.
2. Bathe K.-J. Finite element procedures in engineering analysis. New Jersey: Prentice-Hall. 1982. P.738.
3. Ragulskis M., Kravčenkienė V. Investigation of the oscillatory dynamics of the plate with the control layer of material. Ultragarsas 2003. 1(46). P.20-23.
4. Hearn D., Baker M. P. Computer graphics. Prentice-Hall International. 1986. P.352.
5. Lenkevičius A., Matickas J. Computer graphics. Kaunas: Technologija. 2000. P.210.
6. Manzione P., Nayfeh A. H. Combination resonance of a centrally clamped rotating circular disk. Journal of Vibration and Control. 2001. Vol.7(7). P.979-1001.
7. Bastos S. F., Borges L., Rochinha F. A. Numerical and experimental approach for identifying elastic parameters in sandwich plates. Shock and Vibration. 2002. Vol.9(4). P.193-20.

K. Ragulskis, I. Tiknevičienė, L. Zubavičius, B. Spruogis

Savitojo dažnio statinio valdymo naudojant fizinį netiesiškumą principas

Reziumė

Pasiūlyta supaprastinta skaitmeninė procedūra savųjų reikšmių uždaviniui spręsti, kurioje įvertinama statiniofizinio netiesiškumo įtaka. Nagrinėjamuoju metodu galima statiškai valdyti konstrukcijos savuosius dažnius. Procedūra taikoma plokščios įtemptos būsenos bei plokštelės lenkimo uždaviniams spręsti.

Pateikta spalio 1 d. 2004.03.01